Molecular Pathways in the Cyclotrimerization of Ethyne on Palladium: Role of the C_4 Intermediate

Charles H. Patterson† and Richard M. Lambert*

Contribution from the Department of Chemistry, University of Cambridge, Cambridge CB2 1EP, England. *Received November 24, 1987*

Abstract: A key intermediate of stoichiometry C_4H_4 relevant to the reaction $3C_2H_2 \rightarrow C_6H_6$ on Pd(111) has been isolated on the surface, and its reactions to form benzene and ethene have been investigated. It is shown that *cis*-3,4-dichlorocyclobutene ($C_4H_4Cl_2$) is an effective reagent for seeding the surface with the C_4H_4 intermediate; at temperatures above 150 K, this precursor dissociates to yield two chlorine adatoms and one molecule of the C_4H_4 adsorbed intermediate. The system has been investigated by multiplexed temperature-programmed reaction spectroscopy (MTPRS), LEED, Auger spectroscopy, and work function measurements and with the aid of deuterium labeling. Molecular pathways for the formation of ethene and benzene are proposed.

Homogeneous reactions of ethynes to form benzenes are well known in solution where they are catalyzed by metal complexes.[1,2] In some cases the absence of side reactions and the use of bulky substituents (which reduce reaction rates) have permitted the isolation of intermediates. For example, the complex $[(Ph_3P)_2(C_2H_5)Co]$ catalyzes the cyclotrimerization of C_2Ph_2, and the intermediates $[(Ph_3P)(C_5H_5)(C_2Ph_2)Co]$ and, more interestingly, $[(Ph_3P)(CH_5)(C_4Ph_4)Co]$ have been identified.[1] An apparently analogous process is the heterogeneously catalyzed low-temperature cyclotrimerization of ethyne to benzene on Pd(111). Following the original reports by Tysoe et al.[3,4] and Sesselmann et al.,[5] this unusual and interesting reaction has also been investigated by other workers.[6-8] The molecular pathway involved in the overall $C_2 \rightarrow C_6$ conversion is of particular mechanistic interest: Tysoe et al. have shown that a C_4 intermediate seems to be involved,[4] and in an earlier paper[8] we have demonstrated that benzene formation does not involve any C–H cleavage. It thus seems likely that the reaction proceeds by stepwise addition of three ethyne molecules and that the C_4 intermediate is in fact a species of stoichiometry C_4H_4. Our principal goal was therefore to establish the role of such an intermediate by preparing a surface C_4H_4 species which exhibited the correct activity for benzene formation. Its presence is detected by allowing it to react with coadsorbed C_2H_2 and examining the products. In this article we report on a technique which has been developed for seeding the Pd surface with the relevant C_4 surface intermediate, shown here indeed to be C_4H_4. Detailed investigation of the subsequent chemistry of this species, including its reaction with C_2H_2, shed considerable light on the mechanism of benzene and ethene formation. A subsequent paper will describe the exploitation of this technique in order to permit isolation and examination of the C_4H_4 species by XPS and HREELS.[9]

Experimental Section

The ultrahigh vacuum system and the methods of dosing hydrocarbons and of correcting multiplexed temperature-programmed reaction (MTPR) spectra for benzene fragmentation in the mass spectrometer have been described elsewhere.[8] The MTPR facility was essential for comparing relative yields of benzenes and ethenes from surfaces bearing both H- and D-containing reactants. MTPR experiments were performed using a VG Q7 quadrupole mass spectrometer programmed by an Acorn Atom microcomputer. Up to 14 masses were routinely monitored in a single experiment; each mass channel had a gain (×1, ×2, ×3, or ×4) programmable by means of an analogue switch and inverting operational amplifier which was also controlled by the microcomputer. Switching from channel to channel was approximately 50 Hz and a heating rate of 15 K s^{-1} was employed.

A consideration of all the available evidence suggested that the C_4 intermediate was, in fact, a C_4H_4 entity—now considered to be either adsorbed cyclobutene or perhaps a metallocycle.[9] Accordingly, two very different methods of introducing C_4H_4 to the crystal surface were tried. The first and most direct method involved oxidation of an organometallic complex ($Fe(CO)_3(C_4H_4)$) by ceric ammonium nitrate[10] in a small reaction vessel attached to the vacuum chamber gas line, the object being to introduce the resulting (highly reactive) cyclobutadiene to the crystal surface as quickly as possible. After immediate trapping of the reaction products (C_4H_4 + CO) at liquid nitrogen temperature, CO was distilled off and pumped away before the remaining material was dosed onto the crystal surface via a capillary array. However, subsequent MTPR measurements showed the method to be unsuccessful, probably because of extensive dimerization of the C_4H_4[11] and the presence of residual CO in the dosing gas. In fact, mass spectrometry did indeed reveal the presence of considerable amounts of CO and some C_8H_8 in the dosing gas.

The second method of attempting to generate C_4H_4 on the surface took advantage of the known ability of Pd to abstract Cl from chlorohydrocarbons, the Pd(111)–Cl system having already been characterized.[12] This method proved to be successful; the reagent *cis*-3,4-dichlorobutene ($C_4H_4Cl_2$) deposits Cl(a) on the surface and an organic intermediate which reacts with ethyne to form benzene. The MTPR fingerprint of this reactively formed benzene is essentially identical with that of benzene formed from ethyne alone. Chlorine atoms produced by the dissociative chemisorption of $C_4H_4Cl_2$ form an ordered array on the surface, detectable by LEED, even at 150 K, thereby permitting estimates to be made of the C_4H_4 coverage. These electronegative atoms did not appear to have a major effect on the subsequent reactive behavior of the organic surface species, in line with other results for the ethyne → benzene reaction on this same surface. Thus on Pd(111), (100), (110) it was found that coadsorbed chlorine led to a slight enhancement of ethyne cyclotrimerization at the expense of competing reactions.[13] Our own results for the same reaction on Pd(111)/S show essentially similar behavior.[14]

Results and Discussion

Dissociative Chemisorption of $C_4H_4Cl_2$. The adsorption of

† Present address: Department of Physics, University of Pennsylvania, Philadelphia, PA 19104.

* To whom correspondence should be addressed.

(1) Yamazaki, H.; Hagihara, N. *J. Organomet. Chem.* **1967**, *7*, 22.
(2) Maitlis, P. M. *Pure Appl. Chem.* **1973**, *33*, 489.
(3) Tysoe, W. T.; Nyberg, G. L.; Lambert, R. M. *J. Chem. Soc., Chem. Commun.* **1983**, 623.
(4) Tysoe, W. T.; Nyberg, G. L.; Lambert, R. M. *Surf. Sci.* **1983**, *135*, 128.
(5) Sesselman, W.; Woratschek, B.; Ertl, G.; Kupper, J.; Haberland, H. *Surf. Sci.* **1983**, *130*, 245.
(6) Gentle, T. M.; Muetterties, E. L. *J. Phys. Chem.* **1983**, *87*, 2469.
(7) Rucker, T. G.; Logan, M. A.; Gentle, T. M.; Muetterties, E. L.; Somorjai, G. A. *J. Phys. Chem.* **1986**, *90*, 2703.
(8) Patterson, C. H.; Lambert, R. M. *J. Phys. Chem.* **1988**, *92*, 1266.
(9) Patterson, C. H.; Mundenar, J. M.; Sneddon, L. G.; Gellman, A.; Timbrell, P.; Lambert, R. M., submitted for publication to *Surf. Sci.*
(10) Watts, L.; Fitzpatrick, J. D.; Pettit, R. *J. Am. Chem. Soc.* **1965**, *87*, 3253.
(11) Watts, L.; Pettit, R. *J. Am. Chem. Soc.* **1965**, *87*, 133.
(12) Tysoe, W. T.; Lambert, R. M. *Surf. Sci.* **1988**, *199*, 1.
(13) Logan, M. A.; Rucker, T. G.; Gentle, T. M.; Muetterties, E. L.; Somorjai, G. A. *J. Phys. Chem.* **1986**, *90*, 2709.
(14) Patterson, C. H.; Lambert, R. M.; in preparation.

0002-7863/88/1510-6871$01.50/0

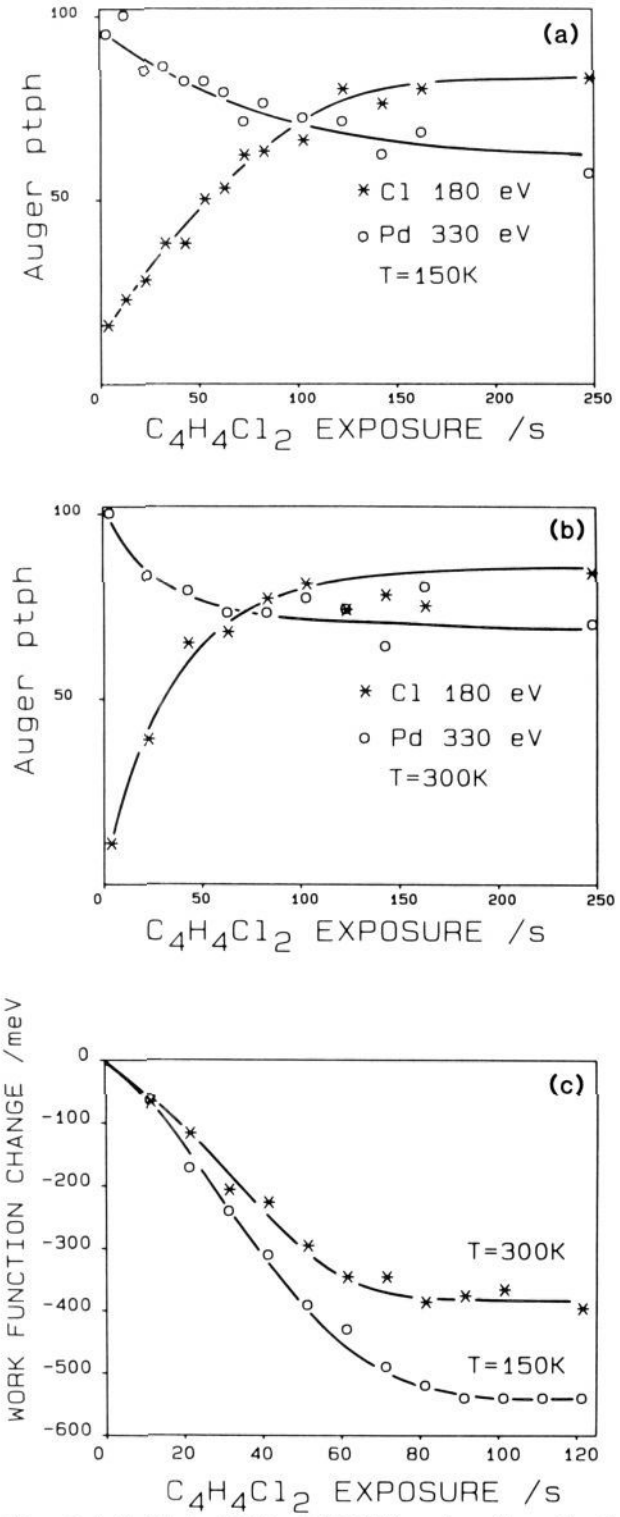

Figure 1. (a,b) Chlorine LMM and Pd LVV Auger intensities and work function change (c) versus $C_4H_4Cl_2$ exposure.

$C_4H_4Cl_2$ on Pd(111) was monitored by Auger spectroscopy (AES), LEED, and work-function change ($\Delta\phi$) at 150 and 300 K. Chlorine 180-eV Auger intensity versus exposure curves are shown in Figure 1a,b, along with the corresponding variations in the Pd 330-eV signal (an exposure of 80 sec using the capillary array doser is equivalent to 1 L; 1 L = 10^{-6} torr s). In both cases, the Cl Auger intensity curves reach a limiting value after approximately 150 s exposure, although the intensity approaches its limiting value more rapidly at 300 K than at 150 K. A corresponding type of behavior was also observed in $\Delta\phi$ measurements

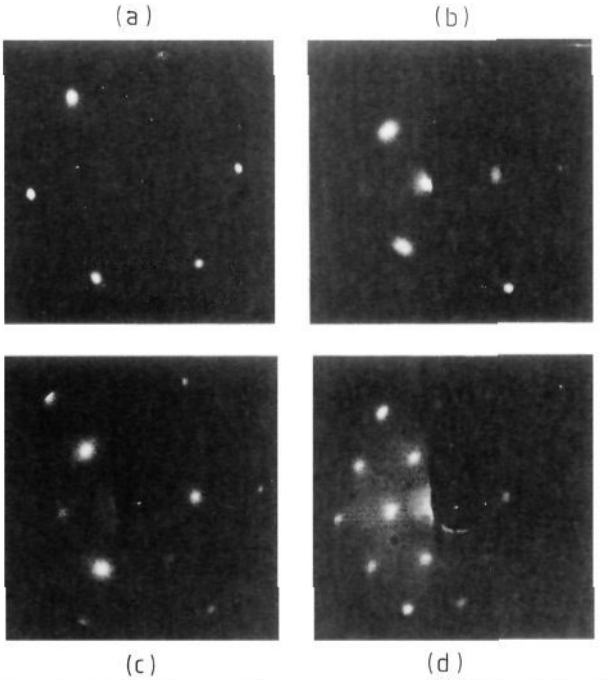

Figure 2. LEED patterns resulting from exposure of Pd(111) to $C_4H_4Cl_2$: (a) clean Pd(111), E_p = 127 eV; (b) 30-s $C_4H_4Cl_2$ dosed at 300 K, E_p = 81 eV; (c) 120-s $C_4H_4Cl_2$ dosed at 150 K then annealed briefly to 440 K, E_p = 81 eV; (d) same as (c) except E_p = 107 eV.

and LEED experiments, a possible explanation being that Cl dissociation limits the rate of adsorption; i.e., adsorption is activated.

Chemisorption of $C_4H_4Cl_2$ causes a monotonic decrease in the work function of Pd(111) which ceases after 90 s exposure at 150 K or 75 s at 300 K (Figure 1c). The limiting $\Delta\phi$ is -0.55 ± 0.02 eV at 150 K and -0.40 ± 0.02 eV at 300 K.

Two different (2 × 2) LEED patterns are observed on adsorbing $C_4H_4Cl_2$ at 300 K; the second pattern appears at a coverage which is equal to twice that required to form the first pattern. The simplest interpretation of these observations is that the first structure corresponds to a (2 × 2) real space net, while the second consists of three coexisting domains of a (2 × 1) real space net. It is argued below that chlorine atoms are the ordered species which are responsible for both structures. Similar behavior is observed in the case of adsorption at 150 K, except that the low coverage (2 × 2) pattern is replaced by a ring pattern whose radius is equal to the (0, $^1/_2$) vector of the (2 × 2) pattern. The high coverage structures formed at 150 and 300 K exhibit the same LEED intensity maxima between 50 and 120 eV, indicating that the ordered adsorbate maintains the same structure over this temperature range. In this work, quoted chlorine coverages are based on the assumption that the LEED patterns are due to ordered Cl atoms.

Development of these LEED patterns with exposure proceeds as follows. At 150 K a faint ring forms after 40 to 50 s exposure, with a radius equal to the distance of the (2 × 2) spots from the specular beam. The ring then gives way to a diffuse (2 × 2) pattern which is brightest after 60 to 70 s and then gradually weakens until 120 s when the pattern has faded completely. On subsequently warming the crystal slowly to 190 K the diffuse pattern reappears, and by 300 K the spots are fairly bright but remain diffuse. Further warming to 440 K results in a sharp, bright (2 × 2) pattern (see Figure 2c,d): annealing for 5 min at this temperature results in the spots fading. For 300 K chemisorption, fairly sharp (2 × 2) spots first appear after 20 s and reach their maximum intensity after 30 s (Figure 2b). However, after 50 s the pattern has weakened considerably. By 70 s the spots have become bright again and reach a maximum intensity at 80 to 90 s; the pattern then becomes weaker until 130 s, when the (2 × 2) spots are very weak indeed. With subsequent gradual

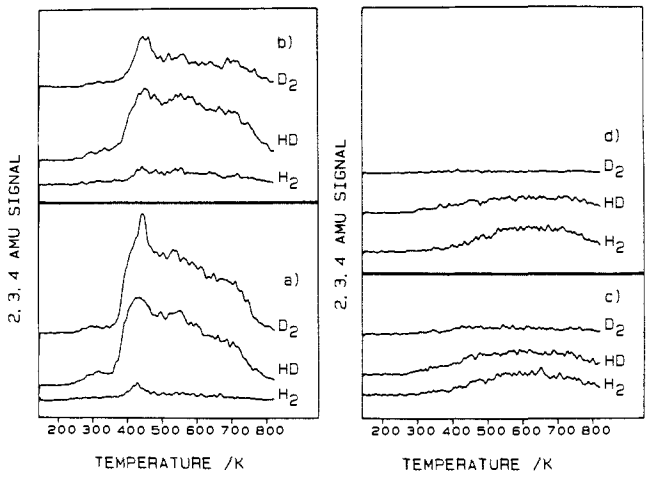

Figure 3. H_2, HD, and D_2 desorption after variable doses of $C_4H_4Cl_2$ at 300 K followed by fixed 40-s doses of C_2D_2 at 150 K: (a)–(d) are for $C_4H_4Cl_2$ preexposures of 30, 60, 80, and 100 s respectively.

heating at this exposure, the spots become sharp between 380 and 390 K. Comparison of the Cl/Pd Auger intensity ratios for the ring and (2 × 2) LEED patterns at 150 or 300 K shows that the low-coverage and high-coverage structures are formed at corresponding coverages at both temperatures; the differences in exposure required to form each structure at the two temperatures presumably arises from differences in sticking probability due to activated adsorption of $C_4H_4Cl_2$ (see above).

Finally, it should be noted that the conclusion that $C_4H_4Cl_2$ adsorption is dissociative with respect to the C–Cl bond, even at low temperatures, is supported by HREEL spectra taken at 205 K and by XP spectra.[9] The former show an intense dipole active loss at 260 cm^{-1} due to a metal-Cl stretching mode. XPS observations on the Cl(2s) level show a 2.1-eV shift to lower binding energies when $C_4H_4Cl_2$ overlayers are heated from 120 to 170 K. This is consistent with the destruction of C–Cl bonds and the formation of metal–Cl bonds.

Reaction Products from MTPR of Coadsorbed $C_4H_4Cl_2$ and C_2D_2. Two series of MTPR experiments were performed with $C_4H_4Cl_2$ and C_2D_2. In the first series, the crystal was exposed to a known, variable dose of $C_4H_4Cl_2$ at 300 K, cooled quickly to 150 K, and then dosed with a fixed amount of C_2D_2. In the second series a similar procedure was followed, except that the temperature was held at 150 K both during the predosing with $C_4H_4Cl_2$ and during the subsequent dosing of C_2D_2. The reaction products monitored were H_2, HD, D_2, $C_2H_xD_{2-x}$, $C_2H_yD_{4-y}$, Cl, $C_6H_zD_{6-z}$, and $C_4H_4Cl_2$; a channel corresponding to C_4H_4 was also monitored but desorption of this species was never detected. The results for H_2, ethene, and benzene production are now described in turn.

a. Hydrogen Desorption. The isotopic distribution in the hydrogen species gives information on the extent to which the adsorbates were dissociated by the surface. Figure 3 shows the raw data for H_2, HD, and D_2 as the relative proportions of $C_4H_4Cl_2$ and C_2D_2 are varied by increasing the precoverage of the former, while Figure 4 summarizes the changes in integrated yields in graphical form. It can be seen that at ~80-s $C_4H_4Cl_2$ preexposure distinct breaks are apparent in the initial rapid decline of both the D_2 and HD yields; correspondingly, a break in the opposite sense is seen for the initially increasing H_2 yield. This critical exposure is also that at which (i) the higher coverage (2 × 2) LEED pattern is completed at 300 K; (ii) the work-function change saturates when $C_4H_4Cl_2$ is adsorbed at 300 K; and (iii) molecular $C_4H_4Cl_2$ desorption becomes apparent when the coadsorption experiment is carried out at 150 K (see below).

These three observations suggest that there is a marked change in the adsorbed layer at around 80-s $C_4H_4Cl_2$ exposure. The C_4H_4 species resulting from dissociative adsorption of $C_4H_4Cl_2$ undergoes reactions both on its own and with coadsorbed C_2D_2 which, among other things, lead to the observed hydrogen profiles. At 150 K and higher initial coverages (>80 s), this dissociative adsorption

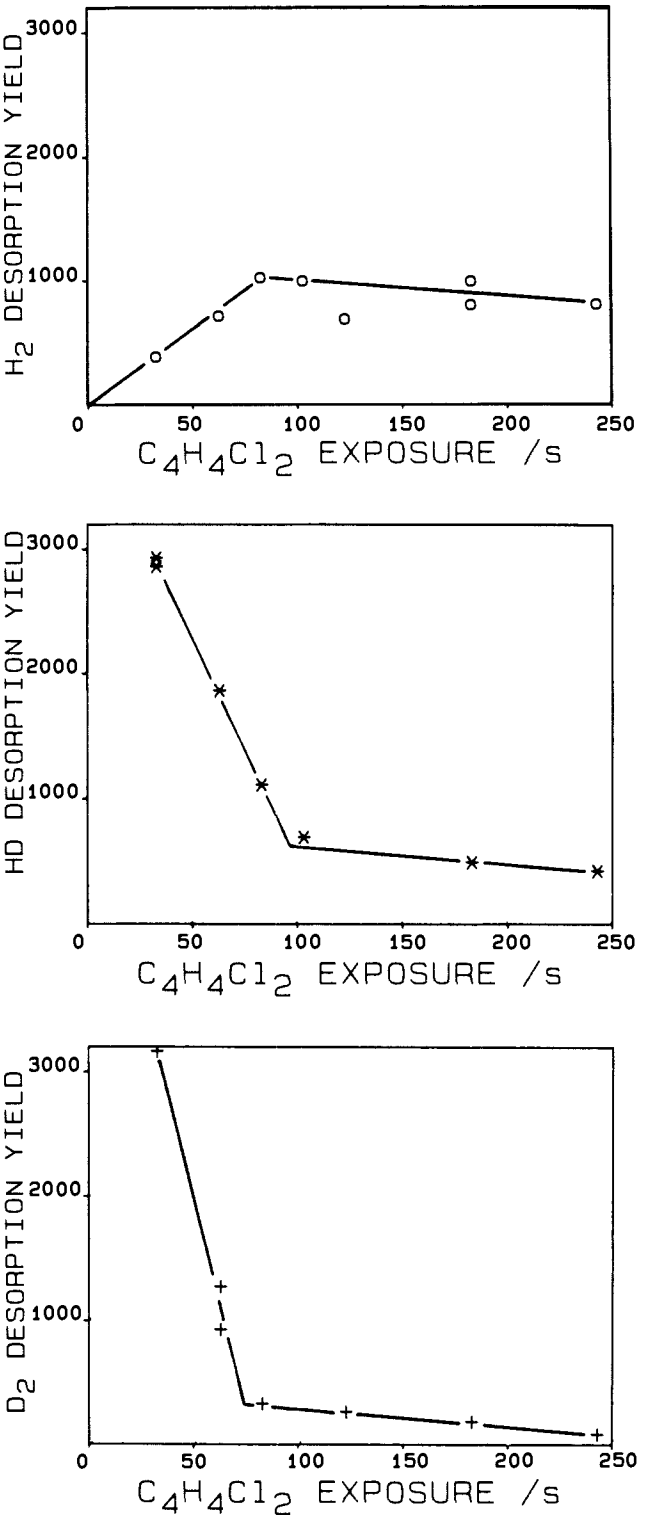

Figure 4. Dependence of H_2, HD, and D_2 integrated desorption yields on preexposure of $C_4H_4Cl_2$ (taken from $C_4H_4Cl_2$ + C_2D_2 data shown in Figure 3).

is prevented, resulting in desorption of $C_4H_4Cl_2$ at 170 K. At either adsorption temperature, surface crowding inhibits some reactions of C_4H_4 and C_2D_2, leading eventually to the suppression of the hydrogen peaks at 300 and 440 K (compare Figure 3, parts b and c).

It is interesting that two very similar hydrogen desorption peaks at ~295 and at ~490 K previously reported[15] for Pt(111) have been ascribed respectively to the formation and decomposition of ethylidyne. Similar hydrogen desorption profiles have *also* been

(15) Salmeron, M.; Somorjai, G. A. *J. Phys. Chem.* **1982**, *86*, 341.

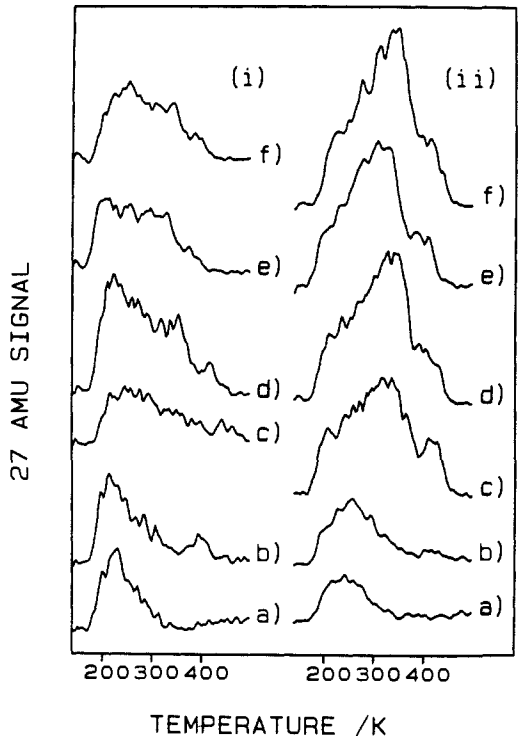

Figure 5. C_2H_4 desorption after variable preexposures of $C_4H_4Cl_2$ at 150 K (series i) or 300 K (series ii) followed by fixed 40-s dose of C_2D_2 at 150 K: (a)–(f) refer to $C_4H_4Cl_2$ exposures of 30, 60, 80, 100, 140, and 180 s respectively.

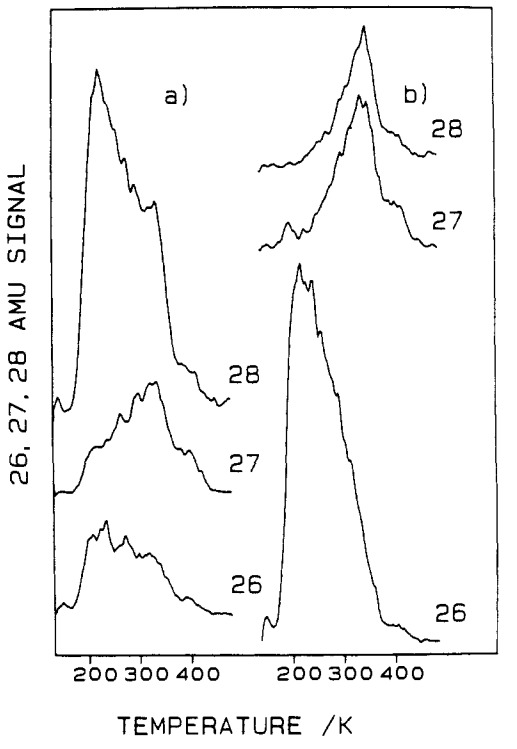

Figure 6. Identification of $C_2H_x^+$ desorption signals by isotopic labeling. 140-s preexposure to $C_4H_4Cl_2$ at 300 K followed by 40 s of either C_2D_2 (a) or C_2H_2 (b) at 150 K.

observed following low-temperature adsorption of C_2H_2 on Pd(111),[3] and HREELS measurements on this same system have detected the formation and decomposition of ethylidyne.[17] The hydrogen desorption peaks observed here are consistent with the formation and decomposition of ethylidyne; they therefore permit the tentative conclusion to be drawn that *both* C_4H_4 and C_2H_2 react to form ethylidyne on Pd(111).

b. Ethene Desorption. Ethene was evolved in both series of $C_4H_4Cl_2 + C_2D_2$ coadsorption experiments and the corresponding ethene desorption spectra are shown in Figure 5. The mass spectra of all hydrocarbons containing more than two carbon atoms exhibit $C_2H_x^+$ ion fragments ($0 < x < 5$) so that deciding the origin of desorption signals at 26, 27, or 28 amu is not straightforward. By comparing relative intensities from reference mass spectra recorded with gaseous samples in the vacuum chamber, and (for a given species) knowing the relative amounts of each higher mass molecule desorbing and the desorption temperatures, it was possible to determine which molecules would contribute significantly to the 26, 27, and 28 amu signals. It emerged that the 27 amu signal was best for determining ethene desorption spectra because the contribution to this signal from other desorbing species was minimal and 27 amu is a major fragment ion of ethene.

For $C_4H_4Cl_2$ exposures <80 s the ethene desorption profiles are qualitatively the same for the two adsorption temperatures (150 and 300 K). However, for $C_4H_4Cl_2$ exposures ≥80 s the behavior depends on the adsorption temperature. The 300 K data exhibit a step increase in the integrated ethene desorption yield and a new ethene peak appears at ~300 K; as already noted, a significant change in hydrogen desorption occurs at the same exposure. All these threshold-type features are absent in the case of $C_4H_4Cl_2$ adsorption at 150 K; a possible explanation for this behavior is given in the next section. Furthermore, by using a method of isotopic substitution described below, *the C_2 skeleton of the ethene was found to have been derived from $C_4H_4Cl_2$, rather than C_2D_2.*

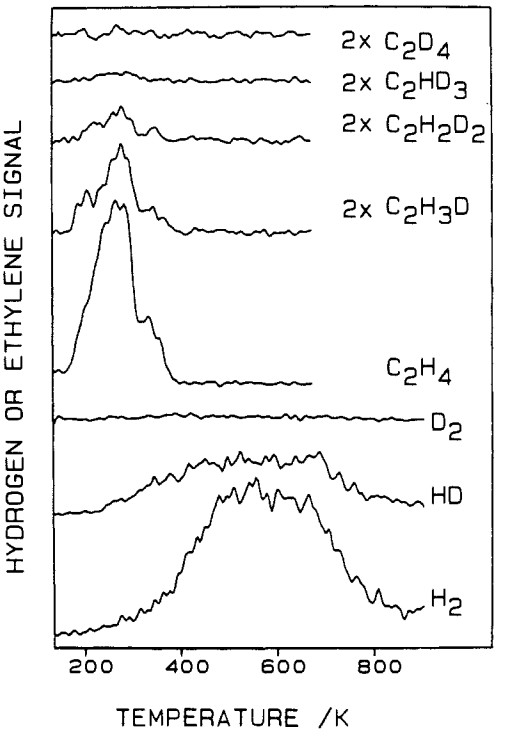

Figure 7. Identification of the source of C_2H_4: 140-s preexposure to $C_4H_4Cl_2$ at 300 K followed by 40-s C_2D_2 at 150 K.

Figure 6a shows a typical set of MTPR spectra from a $C_4H_4Cl_2 + C_2D_2$ coadsorption experiment, the identities of the 26, 27, and 28 amu signals in this being determined by substituting C_2H_2 for C_2D_2 in a further coadsorption experiment in which $C_4H_4Cl_2$ was dosed at 300 K followed by C_2H_2 at 150 K (Figure 6b). In this latter case, the 28 amu signal must be due to $C_2H_4^+$ since there is no deuterium in the system; the peak does not correlate with that from any higher mass molecules giving rise to a 28 amu signal, and so the peak at 27 amu in the $C_4H_4Cl_2 + C_2D_2$ coadsorption

(16) Tysoe, W. T.; Nyberg, G. L.; Lambert, R. M. *J. Phys. Chem.* **1984**, *88*, 1960.
(17) Gates, J. A.; Kesmodel, L. L. *Surf. Sci.* **1983**, *124*, 68.

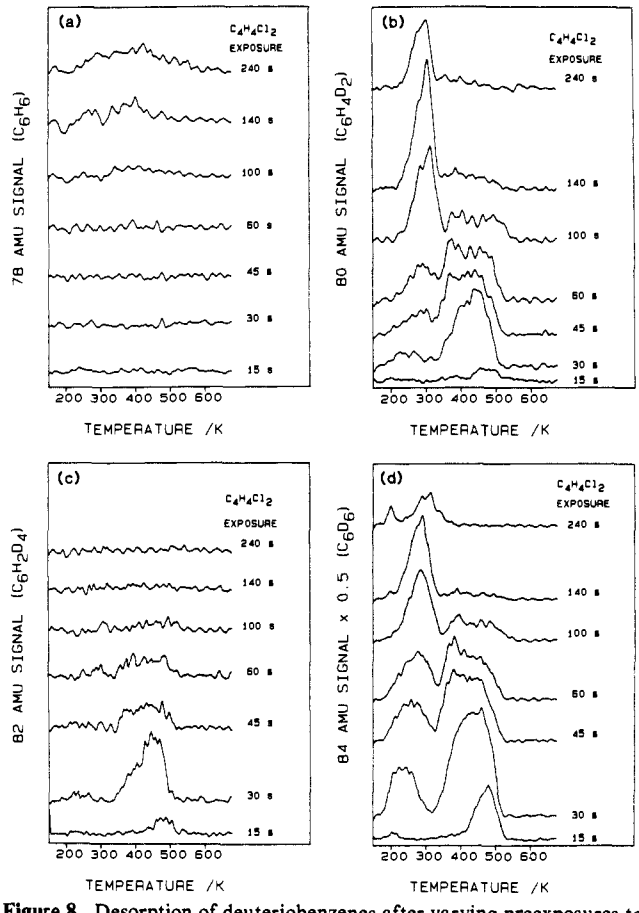

Figure 8. Desorption of deuteriobenzenes after varying preexposures to $C_4H_4Cl_2$ at 150 K followed by 40-s C_2D_2 at 150 K: (a) C_6H_6, (b) $C_6H_4D_2$, (c) $C_6H_2D_4$, (d) C_6D_6 (the MTPR spectra have been corrected for fragment ion interference).

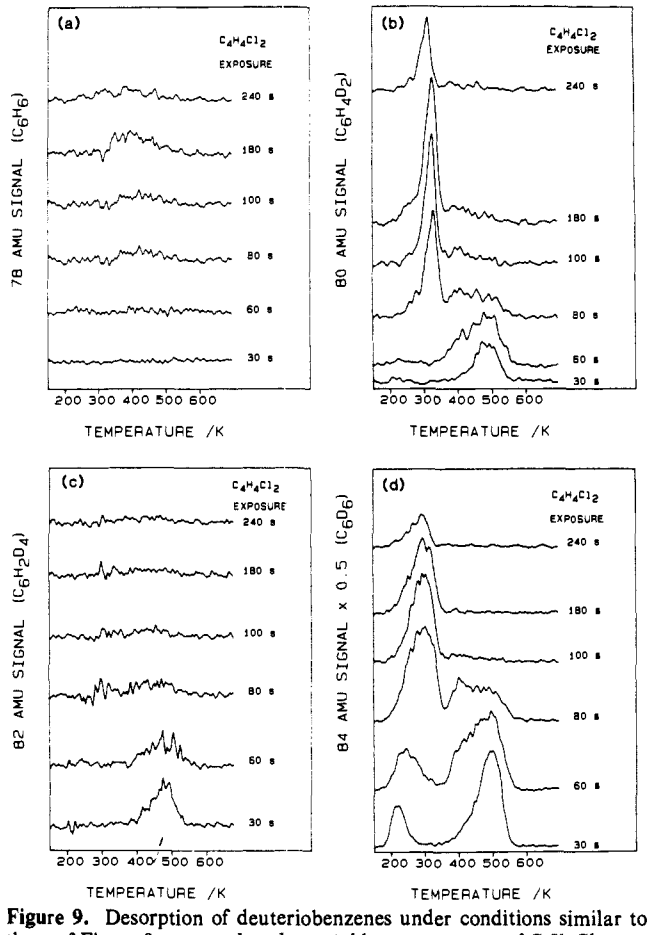

Figure 9. Desorption of deuteriobenzenes under conditions similar to those of Figure 8, *except that the variable preexposures of $C_4H_4Cl_2$ were made at* 300 *K*.

experiment (Figure 6a) may be unambiguously assigned to desorbing ethene. The shape and peak temperature of both these peaks (27 and 28 amu) closely resemble those reported by Tysoe et al.[16] for ethene desorption from ethene adlayers on Pd(111), which further confirms the assignment.

The origin of the carbon skeleton in this reactivity formed ethene can be elucidated from the MTPR spectra of all five ethenes produced by $C_4H_4Cl_2 + C_2D_2$ coadsorption and reaction. If the carbon skeleton of the ethene were derived exclusively from the C_2D_2, no C_2H_4 nor C_2H_3D would be observed except for that formed by H/D exchange in the product ethene. While it is possible that the ethene distribution could arise through H/D exchange, this is considered unlikely on two grounds: (a) the experimental time scale is likely to be too short for equilibration of this relatively inefficient process; and (b) more importantly, the reservoir of surface hydrogen atoms is severely limited by the efficient ethyne (a) → ethene (g) reaction. Figure 7 shows the relevant hydrogen and ethene MTPR profiles. It can be seen that nearly all the ethene formed is C_2H_4 suggesting that the carbon skeleton must be derived from $C_4H_4Cl_2$; molecules containing more than two deuterium atoms are entirely absent. The mechanistic significance of this observation is discussed later.

c. Benzene Desorption. Figures 8 and 9 show selected MTPR spectra for benzene formation resulting from adsorption of varying doses of $C_4H_4Cl_2$ at 150 K (Figure 8) or 300 K (Figure 9). Where appropriate, the spectra have been corrected for fragment ion contributions from the relevant higher mass benzenes. In these experiments we have set out to show that C_4H_4 introduced to the surface via $C_4H_4Cl_2$ is incorporated into the product benzene in a way which suggests that it is a chemical intermediate in the cyclotrimerization of ethyne. If benzene formation proceeds according to the reaction

$$C_4H_4 + C_2D_2 \rightarrow C_6H_4D_2$$

then the only benzene molecules we expect to observe are $C_6H_4D_2$ and C_6D_6 (the latter from C_2D_2 cyclotrimerization). On the other hand, if $C_4H_4Cl_2$ undergoes some dissociation to ethyne, then $C_6H_2D_4$ is indeed observed, *but only in the high-temperature peak and at low $C_4H_4Cl_2$ exposures*. However, it has been shown elsewhere[6,8] that H/D exchange takes place between those benzene molecules which desorb in the high-temperature peak, and we propose that this is the process which gives rise to $C_6H_2D_4$ in the present case (note that no C_6H_6 is observed). In this series of measurements, all seven masses (78–84 amu) were in fact monitored; signals at masses other than 80 amu ($C_6H_4D_2^+$) and 84 amu ($C_6D_6^+$) could all be accounted for in terms of mass spectrometer fragmentation and/or H/D exchange in the high-temperature peak.

It therefore appears that $C_6H_4D_2$ is formed in the initial chemical events and partly desorb in the low-temperature peak; some of the remaining molecules undergo H/D exchange as the temperature is raised, eventually producing new benzenes in the high-temperature peak only. The relative amounts of such exchanged benzenes would depend on the relative amounts of adsorbed H and D in the mixed layer. Figure 4 shows that at low $C_4H_4Cl_2$ exposures the predominant hydrogen species desorbing is D_2 so that D for H exchanged benzenes would be expected to predominate in these circumstances. This is entirely consistent with the observation of some $C_6H_2D_4$ and no C_6H_6 at low $C_4H_4Cl_2$ exposures. Figure 4 provides additional evidence in support of this H/D exchange hypothesis for the production of $C_6H_2D_4$ (as opposed to the alternative explanation involving dissociation of the C_4H_4 intermediate to yield $2C_2H_2$). It shows that C–H scission to yield exchangeable adsorbed reactants is a significant process only at low coverages of reactants, and this is exactly in line with the conditions under which $C_6H_2D_4$ is observed; at higher coverages, production of this molecule is completely suppressed (Figures 8 and 9).

The $C_6H_4D_2$ and C_6D_3 are formed in the initial chemical events and partly desorb in the low-temperature peak; some of the re-

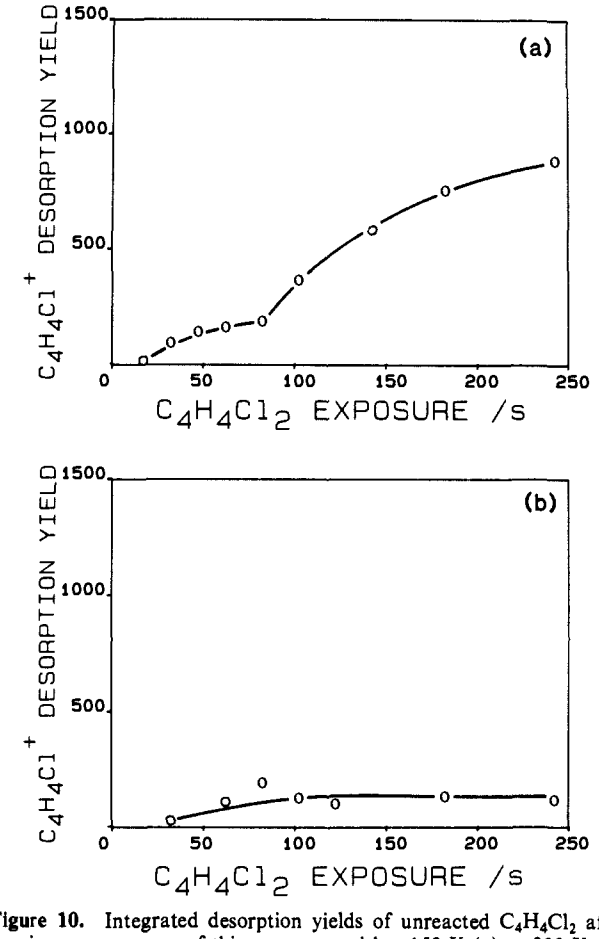

Figure 10. Integrated desorption yields of unreacted $C_4H_4Cl_2$ after varying preexposures of this reagent at either 150 K (a) or 300 K (b), followed by fixed 40-s doses of C_2D_2 at 150 K.

maining molecules undergo H/D exchange as the temperature is raised, eventually producing new benzenes in the high-temperature peak only. The relative amounts of such exchanged benzenes would depend on the relative amounts of adsorbed H and D in the mixed layer. Figure 4 shows that at low $C_4H_4Cl_2$ exposures the predominant hydrogen species desorbing is D_2 so that D for H exchanged benzenes would be expected to predominate in these circumstances. This is entirely consistent with the observation of some $C_6H_2D_4$ and no C_6H_6 at low $C_4H_4Cl_2$ (as opposed to the alternative explanation involving dissociation of the C_4H_4 intermediate to yield $2C_2H_2$). It shows that C–H scission to yield exchangeable adsorbed hydrogen is a significant process only at low coverages of reactants, and this is exactly in line with the conditions under which $C_6H_2D_4$ is observed; at higher coverages, production of this molecule is completely suppressed (Figures 8 and 9).

The $C_6H_4D_2$ and C_6D_6 spectra observed here do not evolve as a function of exposure in the same way as those for benzene from C_2H_2 alone.[3,8] In the latter case both high- and low-temperature peaks grow together with increasing ethyne exposure. In the present case the $C_6H_4D_2$ and C_6D_6 spectra *always mirror one another*, but their evolution with coverage is different from that observed for the simple $C_2H_2 \rightarrow C_6H_6$ system. Their parallel behavior here demonstrates the important point that there is no kinetic barrier for formation and desorption of $C_6H_4D_2$ (from $C_4H_4 + C_2D_2$) greater than any encountered in the pathway $3C_2D_2 \rightarrow C_6D_6$. Earlier work has shown[8] that the evolution of C_6H_6 from C_2H_2 on clean Pd(111) is desorption rate limited rather than reaction rate limited. The processes involved in the two cases are:

$$2C_2D_2 \xrightarrow{+C_2D_2} C_4D_4 \rightarrow C_6D_6$$

$$C_4H_4Cl_2 \xrightarrow{+C_2D_2} C_4H_4 \rightarrow C_6H_4D_2$$

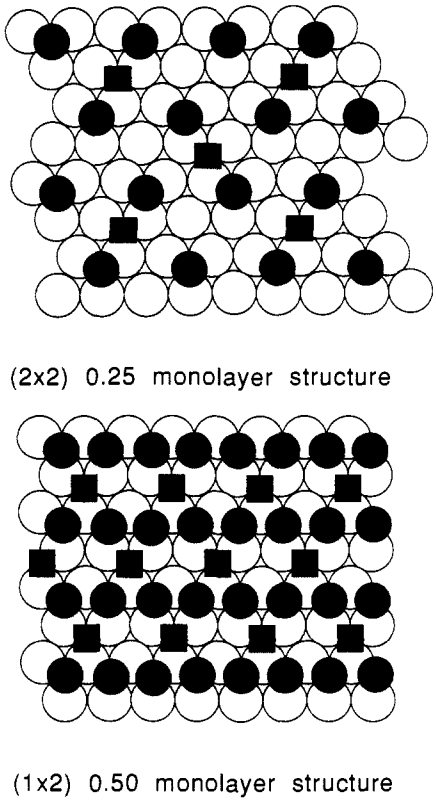

Figure 11. Postulated structures for the $^1/_4$Cl monolayer and $^1/_2$Cl monolayer phases: open circles, Pd; filled circles, Cl atoms; hatched squares, hydrocarbon moiety.

The coverage dependence of the spectra reported here *is*, however, very similar to that observed for benzene formation on Pd(111) surfaces predosed with sulfur;[14] the relative amount of benzene desorbing in the low-temperature peak is increased compared to the clean metal surface case. It therefore seems reasonable to suggest that adsorbed Cl (resulting from $C_4H_4Cl_2$ decomposition) acts in an analogous way to adsorbed S, possibly by inhibiting formation of the "flat-lying" benzene which is associated with the high-temperature peak.

d. Fate of Unreacted $C_4H_4Cl_2$ and Residual Chlorine. Figure 10a,b shows the integrated desorption yield of unreacted $C_4H_4Cl_2$ (monitored at 87 amu) from the mixed adsorption layer. Desorption of this molecule occurs in a single narrow peak (fwhm = 60 K) centered at 170 K only when $C_4H_4Cl_2$ is adsorbed at 150 K (this is *not* associated with the desorption of multilayers of physisorbed $C_4H_4Cl_2$); HREELS data[9] show that such layers are formed below 130 K. We therefore associate this peak $C_4H_4Cl_2$ associatively adsorbed on Pd(111). The break in the yield curve at ~80-s exposure (Figure 10a) coincides with the coverage at which the intensity of the (2 × 2)-Cl LEED pattern is maximized. It therefore suggests that beyond this coverage $C_4H_4Cl_2$ adsorbs at low temperature with relatively little dissociation.

Chlorine desorption spectra following $C_4H_4Cl_2$ or $C_4H_4Cl_2 + C_2D_2$ adsorption were very similar to those found for chlorine overlayers on Pd(111),[12] desorption occurring exclusively as atomic chlorine. This observation, combined with the temperature dependence of the (2 × 2) LEED pattern, strongly suggests that dissociation of $C_4H_4Cl_2$ occurs well below 300 K to yield C_4H_4 and Cl. With increasing temperature, the former species undergoes reaction while the latter merely desorbs, fading of the (2 × 2) LEED pattern correlating with desorption of Cl (this work). These results therefore indicate that $C_4H_4Cl_2$ adsorbs on Pd(111) with partial dissociation even at 150 K to yield C_4H_4(a) and chemisorbed Cl. On raising the temperature, intact $C_4H_4Cl_2$ desorbs at ~170 K leaving the C_4H_4(a) to undergo hydrocarbon reactions in the presence of Cl(a), this latter species eventually desorbing as chlorine atoms.

Summary and Conclusions

The LEED intensity data reveal that *two* ordered phases are formed on adsorbing $C_4H_4Cl_2$ at both 150 and 300 K. While it is possible that the mixed overlayer involves long-range ordering of both the hydrocarbon species and chlorine, this interpretation is made less likely by the observed temperature dependence. In particular, the structure persists in a temperature regime where extensive hydrocarbon reactions are occurring. Therefore, the simplest interpretation is that the first pattern to appear corresponds to a (2 × 2) chlorine mesh (Cl coverage = 1/4). The second pattern could then be assigned to a (2 × 1) chlorine phase (Cl coverage = 1/2) which is present as three symmetry-related domains. This view is confirmed by recent HREELS measurements.[9] Possible surface structures are indicated in Figure 11, the important point being that completion of the second structure is found to occur just before the coverage at which dissociation of $C_4H_4Cl_2$ is substantially inhibited.

Before proceeding to a consideration of the mechanism of benzene formation, it is worth noting that the present results shed some useful light on the mode of ethene formation in the system. Earlier work has suggested that on Pd(111) vinylidene is the intermediate which is formed from ethyne and which eventually undergoes hydrogenation to ethene.[4] Here, we observe that C_2H_4 is desorbed in a similar fashion when C_4H_4 rather than C_2H_2 is the species initially present on the surface; a possible new route from ethyne to ethene (via C_4H_4) appears to be indicated. However, HREELS data[9] show that C_4H_4 rearranges to vinylidene at a temperature below that at which C_2H_4 desorbs, so that even this pathway involves the formation of a vinylidene intermediate.

The ethene desorption profiles measured for $C_4H_4Cl_2 + C_2D_2$ coadsorption experiments showed an interesting coverage dependence when $C_4H_4Cl_2$ was adsorbed at 300 K; only a small amount of ethene desorbs below 300 K for $C_4H_4Cl_2$ exposures <70 s, but above this exposure the yield of desorbing ethene rapidly increases and the C_2H_4 peaks shifts to 350 K. The hydrogen species desorption profile also changes markedly between these two cases; the sharp leading edge of the low $C_4H_4Cl_2$ exposure experiments at 450 K is removed and a much flatter desorption profile is observed.

We postulate that the switch in behavior is due to the formation of ethylidyne rather than vinylidene from C_4H_4 when the surface coverage is low. This conclusion is supported by HREELS measurements on the decomposition of C_4H_4.[9]

A principal object of this work was better understanding of the mechanism of ethyne cyclotrimerization on Pd(111), and evidence has been presented that $C_4H_4Cl_2$ acts as a reagent for depositing C_4H_4(a) species on the surface. The results of the $C_4H_4Cl_2 + C_2D_2$ experiments establish that the C_4H_4 moiety is built directly into the product benzene as C_4H_4 rather than $2C_2H_2$; this is demonstrated by the observed isotopic distribution. Futhermore, the C_6D_6 "by-product" which is formed in these experiments shows a MTPR profile which exactly mirrors that of the $C_6H_4D_2$. This demonstrates that the two kinds of benzene are formed by routes which are very closely related; indeed they are energetically indistinguishable in these experiments:

$$3C_2D_2(a) \rightarrow C_6D_6$$

and

$$C_4H_4(a) + C_2D_2(a) \rightarrow C_6H_4D$$

appear to be equivalent pathways. Control experiments show that the high-temperature benzene peak is associated with molecules which are chemisorbed in the same state as those resulting from the direct adsorption of benzene, i.e., "flat-lying". The low-temperature peak is accordingly assigned to the desorption of a less strongly bound mode of reactivity formed benzene (i.e., "tilted") generated on an initially crowded surface. The effect of surface chlorine is to increase the relative amount of reactively formed benzene desorbing at low temperature, with a concomitant narrowing and upward shift of the associated desorption peak. The overall scheme of hydrocarbon reactions can therefore be illustrated as shown in Scheme I.

Scheme I

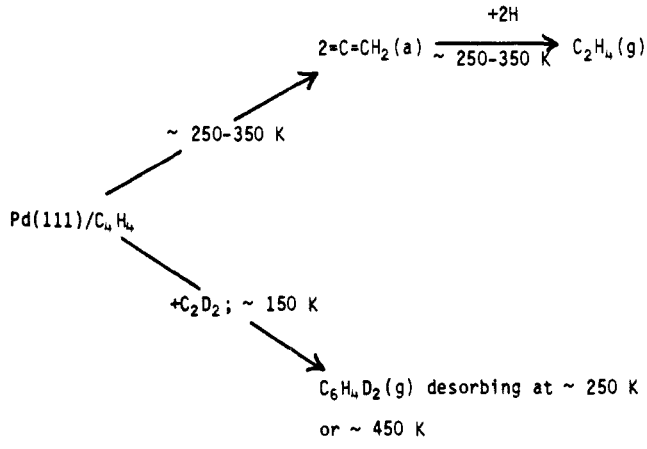

Acknowledgment. C.H.P. thanks the Department of Education of Northern Ireland for the award of a research studentship. We are grateful for Johnson Matthey Ltd. for a loan of precious metals and to R. Stevenson for assistance with the synthesis of cyclobutadiene iron tricarbonyl.

Registry No. C_2H_2, 74-86-2; Pd, 7440-05-3.

Communications to the Editor

Isolation and X-ray Crystal Structure of the First Dinitrogen Complex of an f-Element Metal, $[(C_5Me_5)_2Sm]_2N_2$

William J. Evans,* Tamara A. Ulibarri, and Joseph W. Ziller

Department of Chemistry, University of California Irvine, California 92717

Received April 6, 1988

Since the discovery of the first dinitrogen complex,[1] $[Ru(NH_3)_5N_2]^{2+}$, there has been extensive research on the synthesis of N_2 complexes and the conversion of the N_2 ligand to NH_3.[2-5] Although many elements are now known to form dinitrogen complexes, a well-characterized N_2 complex of an f-element metal

(1) Allen, A. D.; Senoff, C. V. *J. Chem. Soc., Chem. Commun.* **1965**, 621–622.
(2) Pelikan, P.; Boca, R. *Coord. Chem. Rev.* **1984**, *55*, 55–112, and references therein.
(3) Henderson, R. A.; Leigh, G. J.; Pickett, C. J. *Adv. Inorg. Chem. Radiochem.* **1983**, *27*, 198–291, and references therein.
(4) Chatt, J.; Dilworth, J. R.; Richards, R. L. *Chem. Rev.* **1978**, *78*, 589–625.
(5) Dilworth, J. R.; Richards, R. L. In *Comprehensive Organometallic Chemistry*; Wilkinson, G., Stone, F. G. A., Abel, E. W., Eds.; Pergamon: Oxford, England, 1982; Chapter 60.

0002-7863/88/1510-6877$01.50/0